Behaviour of rays near S-wave singularities in anisotropic media

Václav Vavryčuk

Geophysical Institute, Academy of Sciences of the Czech Republic, Boční II/1401, 141 31 Praha 4, Czech Republic. E-mail: vv@ig.cas.cz

SUMMARY

The behaviour of rays can display a complicated pattern near singularities in inhomogeneous anisotropic media. The peculiarities in the ray field arise particularly near the conical and wedge singularities, which generate linear, circular or elliptical anticaustics in their vicinities. The anticaustics represent barriers for rays and prevent the rays from crossing them. If the rays approach the anticaustic, they can be strongly curved and deflected from their original direction. The rays outside the anticaustic are forced to move around the anticaustic. The rays inside the anticaustic are captured and forced to pass the caustic generated by the singularity. The anomalies in the ray behaviour are more pronounced under strong anisotropy, if anisotropy decreases the ray field becomes more regular.

1. INTRODUCTION

Singularities are directions in anisotropic media in which two or three waves have coincident phase velocities. These directions are extremely important because they can cause anomalies in the field of polarization vectors (Alshits, Sarychev & Shuvalov 1985; Shuvalov 1998) and in the geometry of the slowness and wave surfaces (Grechka & Obolentseva 1993; Shuvalov & Every 1996, 1997; Vavryčuk 2002). For example, the Gaussian curvature of the slowness surface can be infinite or it may not be even defined in the singularity. The singularities can appear in weakly as well as in strongly anisotropic media and they are usually connected with the presence of caustics. The caustics complicate the geometry of rays, but do not pose complications in ray-tracing equations. However, the singularities often cause trouble in tracing rays. Since the medium is degenerate in singularities, the standard ray-tracing equations in anisotropic media (Červený 1972; Červený, Molotkov & Pšenčík 1977; Gajewski & Pšenčík 1990; Červený 2001) produce numerical instabilities or they even fail whenever the ray approaches the near-singularity directions (Pšenčík & Dellinger 2001). So far these complications prevented to study the geometry of rays in these directions, hence it is little known about the behaviour of rays in anisotropy with singularities.

In this paper, the behaviour of rays is studied in the vicinity of singularities in inhomogeneous anisotropic media by applying the ray-tracing algorithm developed by Vavryčuk (2001). The developed algorithm is a slight modification of the ray tracing based on evaluating the right-hand sides of equations using the polarization vectors of the traced wave. The algorithm is numerically stable and yields correct results when tracing rays in anisotropic media with all kinds of singularities. This enables us to address particularly the following points: Can a ray touch or cross the singularity? Is the geometry of the ray field affected by the singularity? How differ the ray fields for various kinds of singularities? Is the ray field affected by caustics and anticaustics associated with the singularity? How differ the ray fields under weak and strong anisotropies?

2. RAY TRACING IN ANISOTROPIC MEDIA WITH SINGULARITIES

Ray-tracing equations for anisotropic inhomogeneous media are expressed as follows (Vavryčuk 2001, Eq. 7):

$$\frac{dx_i}{d\tau} = a_{ijkl}\, p_l\, g_j\, g_k\,, \quad \frac{dp_i}{d\tau} = -\frac{1}{2}\frac{\partial a_{jkln}}{\partial x_i}\, p_k\, p_n\, g_j\, g_l\,. \tag{1}$$

where $\mathbf{x}$ is the position vector, τ is the traveltime, $\mathbf{p} = \dfrac{\partial \tau}{\partial \mathbf{x}} = \dfrac{\mathbf{n}}{c}$ is the slowness vector, $\mathbf{n}$ is the slowness direction, c is the phase velocity, $\mathbf{g}$ is the polarization vector, and a_{ijkl} is the density-normalized elasticity tensor. Polarization vector $\mathbf{g}$ is calculated from

$$\Gamma_{jk}\, g_k = G\, g_j\,, \tag{2}$$

where

$$\Gamma_{jk}(\mathbf{n}) = a_{ijkl}\, n_i\, n_l\,. \tag{3}$$

Christoffel tensor $\Gamma_{jk}(\mathbf{n})$ has three eigenvalues G, which are real-valued and positive ($G = c^2$), and three eigenvectors $\mathbf{g}$. The eigenvalues correspond to three waves (P, $S1$ and $S2$) propagating in anisotropic media, and the eigenvectors correspond to the polarization vectors of these three waves.

Equations (1) and (2) can be readily used for tracing rays outside singularities. Since the Christoffel tensor is non-degenerate, polarization vector $\mathbf{g}$ is determined uniquely from (2) and the right-hand sides of (1) are evaluated without difficulties. However, if the medium contains singularities, Eqs (1) and (2) are not sufficient for tracing rays. Since, the Christoffel tensor is

degenerate in singularities, Eq. (2) yields ambiguous solution for **g**. Hence, we cannot evaluate uniquely the right-hand sides of (1). In this case, Eqs (1) and (2) must be complemented by an additional condition requiring the polarization vector of the traced wave to be continuous along a ray (see Vavryčuk 2001).

3. BEHAVIOUR OF RAYS NEAR SINGULARITIES

We shall study the behaviour of rays near the kiss, conical and wedge singularities (Shuvalov 1998). We shall show that the behaviour of rays is mainly controlled by the shape of the slowness and wave surfaces that can be rather complicated near the singularities. Some of the singularities studied will be touched or crossed by parabolic lines. These lines are formed by points with the zero Gaussian curvature of the slowness surface and separate convex, concave and saddle-shaped areas on this surface. The parabolic lines on the slowness surface map into caustics on the wave surface, which are formed by cusped edges with the infinite Gaussian curvature. The cusped edges can occur also on the slowness surface and define the conical and wedge singularities. These singularities display the infinite Gaussian curvature of the slowness surface and are mapped into anticaustics on the wave surface, which are defined by the zero Gaussian curvature. Since the singularities are very often connected with the caustics and anticaustics, the ray field will be studied in presence of all these phenomena.

The behaviour of rays will be demonstrated using equal-area plots. These plots transform each direction of a ray into a point inside a circle (see Fig. 1). The centre of the circle corresponds to the vertical direction. The points at the circle correspond to a constant deviation of rays from the vertical axis. The position of the point is calculated from the ray direction as follows (see Aki & Richards 1980, Fig. 4.17):

$$x = \sin\frac{\theta}{2}\cos\phi\,,\quad y = \sin\frac{\theta}{2}\sin\phi\,, \tag{4}$$

where θ is the deviation of the ray from the vertical axis, and ϕ is the polar angle of the ray direction defined in the horizontal plane. If the ray is a straight line, then it projects into one point in the equal-area plot. If the ray is bend due to the gradient in the medium, the ray projects into a curve.

3.1. Kiss singularity

The kiss singularity arises if the slowness sheets of two waves touch tangentially at an isolated point. The typical kiss singularity occurs along the rotational symmetry axis in transverse isotropy and along symmetry axes in cubic and tetragonal symmetries (see Vavryčuk 1999, 2002). The topological charge of the field of polarization vectors in the singularity can attain values 0, +1 or –1 (see Shuvalov 1998). The shape of the slowness sheets can display

irregularities in the singularity: the slowness sheets can be differentiated at the first order only and the Gaussian curvature may not be defined in the singularity (Shuvalov & Every 1996; Vavryčuk 2002). The kiss singularity can even be touched by parabolic lines on the slowness surface and by caustics on the wave surface.

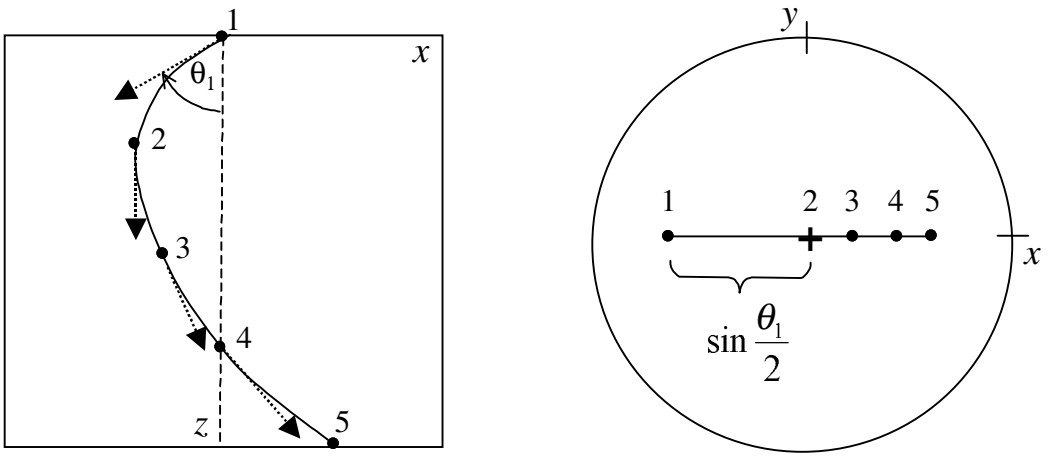

Figure 1. The representation of a ray (left) in the equal-area projection (right). The centre of the circle (marked by the cross) coincides with the vertical axis. The circle corresponds to a constant deviation of ray directions from the vertical axis. The full dots mark the points at a ray (left) and corresponding directions (tangents) of a ray at these points (right).

We shall consider two anisotropy models (see Fig. 2): (a) transverse isotropy and (b) cubic anisotropy. Both models are inhomogeneous with a constant velocity gradient ε along the x-axis. The source of wave is situated at the origin of coordinates. The elastic parameters are at the source: (a) $a_{11}=a_{22}=a_{33}=6.25$, $a_{44}=a_{55}=a_{66}=2.50$, $a_{12}=1.25$, $a_{13}=a_{23}=4.50$, and (b) $a_{11}=a_{22}=a_{33}=6.25$, $a_{44}=a_{55}=a_{66}=2.08$, and $\gamma=a_{12}-a_{11}+2a_{44}=2.00$. Parameter γ is the measure of the strength of anisotropy. The elastic parameters at other points of the medium were calculated as follows:

$$a_{kl}(x)=a_{kl}(x_0)(1+\varepsilon\, x)^2, \tag{5}$$

where $a_{kl}(x_0)$ are the density-normalized elastic parameters at the source in the Voigt notation, and gradient ε equals 0.01. Anisotropy in both models is rather strong, hence wave surfaces form triplications (see Fig. 2).

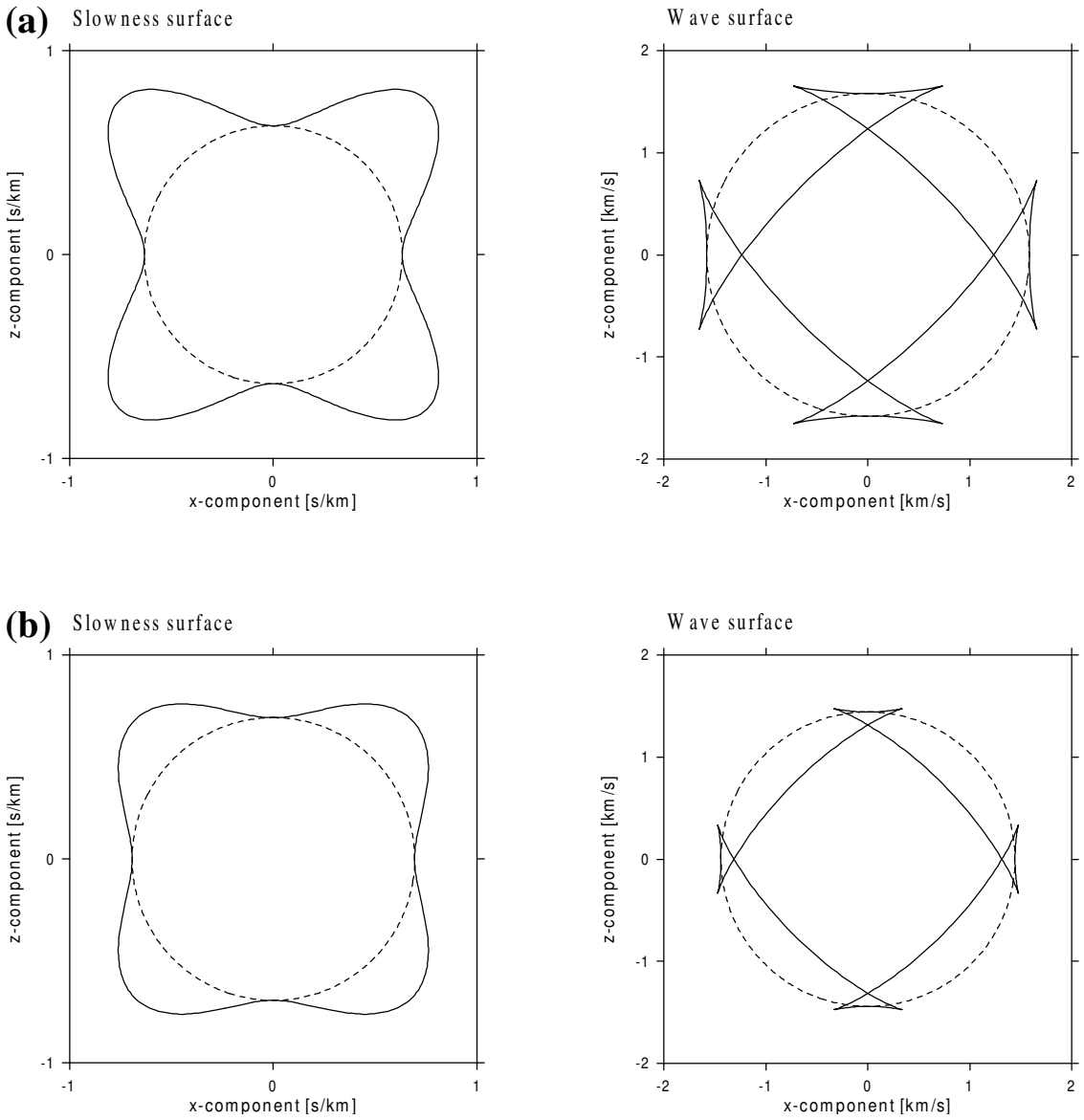

Figure 2. The sections of the slowness and wave surfaces for anisotropic models (a) and (b) in the *x*-*z* plane. The dashed and full lines denote the slowness and wave sheets of the *S*1 and *S*2 waves, respectively. For parameters of the (a) and (b) models, see the text.

Anisotropy model (a) generates a kiss singularity along the vertical axis. The topological charge of the field of polarization vectors is +1 in the singularity. The shapes of the slowness and wave sheets in the singularity and its vicinity are convex for the fast *S* wave, but concave for the slow *S* wave. The rays were shot from the source in the following angular interval: $\vartheta = 5°$, $\varphi \in \langle -40°, 40° \rangle$ in steps of 4°, where ϑ is the deviation of the slowness vector from the vertical axis, and φ is the polar angle of the slowness vector.

Figure 3 shows the equal-area projection of rays near the kiss singularity in model (a) for fast and slow *S* waves. The gradient in the medium is along the *x*-axis and causes that rays are not straight lines, but they change their directions in time. Figure 3 shows that the change of the ray directions is along the *x*-axis for both *S* waves, hence it follows the direction of the gradient in the medium. However, the change of the ray directions has an opposite sign for both *S* waves. This is caused by different shapes of the slowness sheets near the singularity: the slowness sheet is convex for the fast *S* wave but concave for the slow *S* wave. No other irregularities are observed in the ray field. Hence one can conclude that the ray field is fully controlled by the gradient in the medium and the kiss singularity induces no effects or anomalies in the ray field.

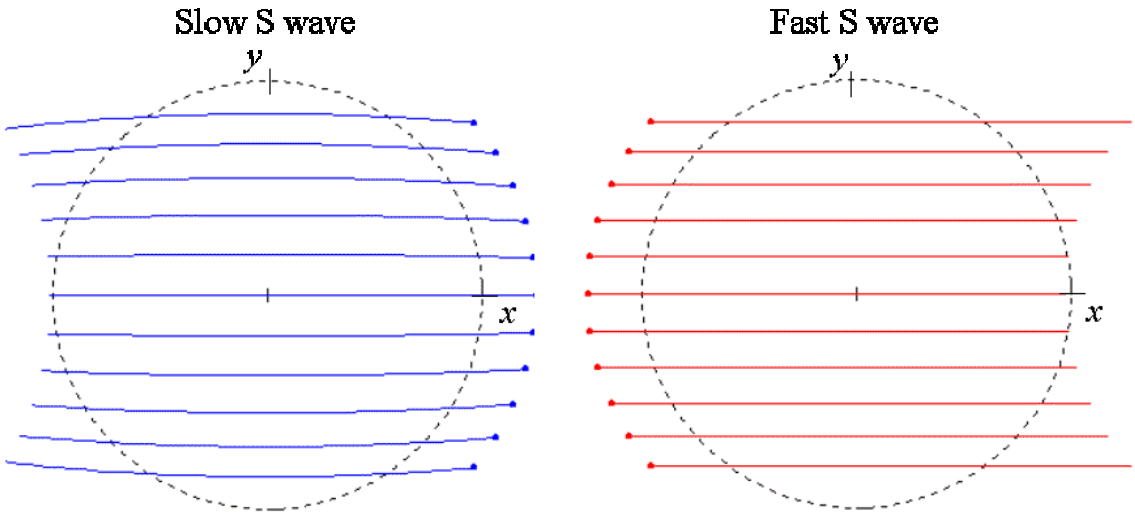

Figure 3. The behaviour of rays near the kiss singularity in model (a). Equal area projection is used. The cross marks the kiss singularity that coincides with the vertical axis. The left/right circle corresponds to the deviation 10°/4° of ray directions from the vertical axis. The full dots mark the initial directions of the rays.

Anisotropy model (b) generates a kiss singularity also along the vertical axis. The topological charge of the field of polarization vectors is +1 in the singularity. The shapes of the slowness and wave sheets are more complex in model (b) than in model (a). The slowness and wave sheets are not smooth and the Gaussian curvature is not defined in the singularity. Moreover, the singularity is touched by parabolic lines on the slowness surface and by caustics on the wave surface (see Fig. 4, upper plots). The rays were shot from the source in the following angular interval: $\vartheta = 16°$, $\varphi \in \langle -40°, 40° \rangle$ in steps of 5°, where ϑ is the deviation of the slowness vector from the vertical axis, and φ is the polar angle of the slowness vector.

Figure 4 (lower plots) shows the equal-area projection of rays near the kiss singularity in model (b) for fast and slow *S* waves. The behaviour of rays near the singularity is rather complex. Rays do not follow the direction of the velocity gradient in the medium as in model (a), but they can significantly deviate from this direction forming complicated 3-D curves. The ray field is also affected by caustics occurring around the singularity and touching the singularity (see Fig. 4, upper plots).

3.2. Conical singularity

The conical singularity arises if two slowness sheets touch through vertices of cone-shaped surfaces (Rümpker & Thomson 1994; Shuvalov 1998). The singularity on the slowness surface generates a caustic and anticaustic on the wave surface. The anticaustic is circular or elliptical. The size of the anticaustic depends on the strength of anisotropy. The semi-axes of the anticaustic increase with increasing the strength of anisotropy. The singularity can be crossed by parabolic lines on the slowness surface. This generates a caustic touched by an anticaustic at isolated points.

The behaviour of rays near a conical singularity is studied in two anisotropic models (see Fig. 5): (c) transverse isotropy and (d) cubic anisotropy. Both models are inhomogeneous with constant velocity gradient $\varepsilon = 0.01$ along the *x*-axis. The source of wave is situated at the origin of coordinates. The elastic parameters are at the source: (c) $a_{11} = a_{22} = a_{33} = 6.00$, $a_{44} = a_{55} = a_{66} = 3.00$, $a_{12} = a_{11} - 2a_{66} = 0$, $a_{13} = a_{23} = 0$, and (d) $a_{11} = a_{22} = a_{33} = 6.25$, $a_{44} = a_{55} = a_{66} = 2.08$, and $\gamma = a_{12} - a_{11} + 2a_{44} = 2.00$. The elastic parameters at other points of the medium were calculated using Eq. (5).

Anisotropy (c) is transverse isotropy with a vertical symmetry axis (see Fig. 5, upper plots). This transverse isotropy is, however, very special, because it forms a conical singularity along the symmetry axis (see Payton 1992), instead of the kiss singularity usually observed under this symmetry. The conical singularity generates a caustic and an anticaustic. The caustic is along the symmetry axis. The anticaustic is circular. The ray directions at the anticaustic deviate from the symmetry axis by angle $\vartheta = 26.56°$. The rays were shot from the source in the following angular interval: $\vartheta = 15°$, $\varphi \in \langle -50°, 50° \rangle$ in steps of 10°, where ϑ is the deviation of the slowness vector from the vertical axis, and φ is the polar angle of the slowness vector.

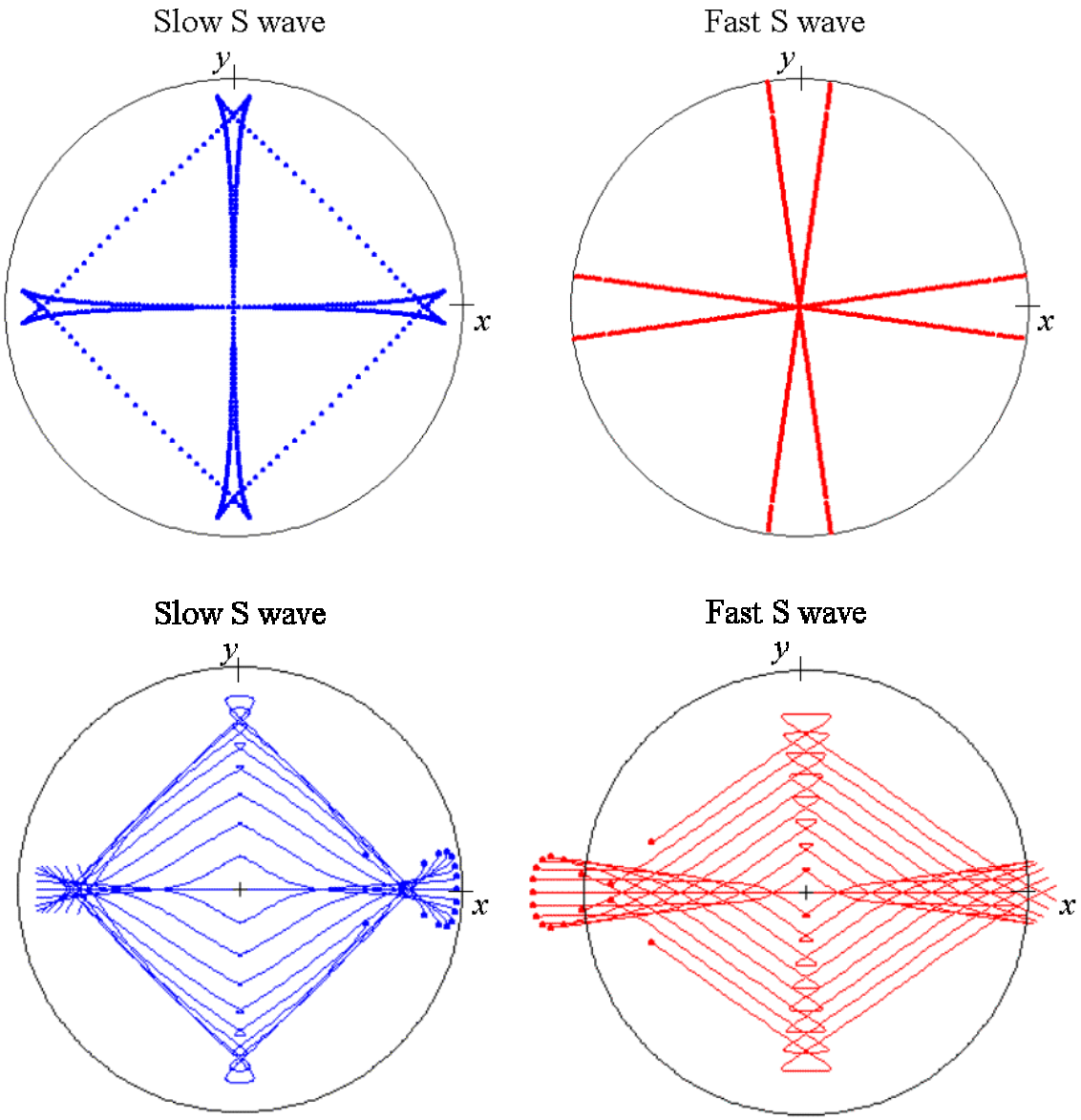

Figure 4. The behaviour of rays (upper plots) and the form of caustics (lower plots) near the kiss singularity in model (b). Equal area projection is used. The cross marks the kiss singularity that coincides with the vertical axis. The circles correspond to the deviation 13° of ray directions from the vertical axis. The full dots in the upper plots mark the initial directions of the rays.

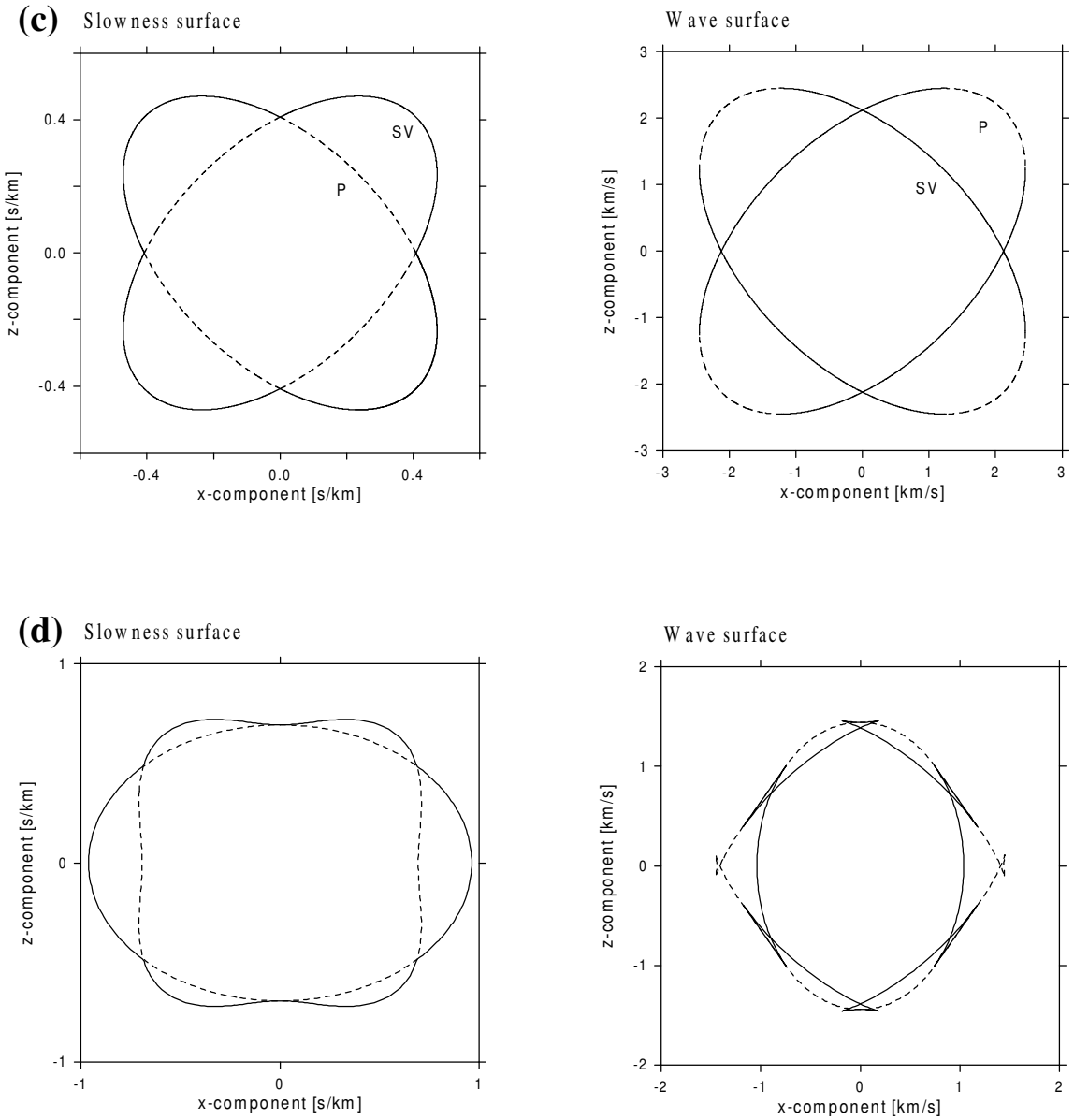

Figure 5. The sections of the slowness and wave surfaces for anisotropic models (c) and (d) in the *x*-*z* plane. The dashed and full lines denote the slowness and wave sheets of the fast and slow waves, respectively. For parameters of the (c) and (d) models, see the text.

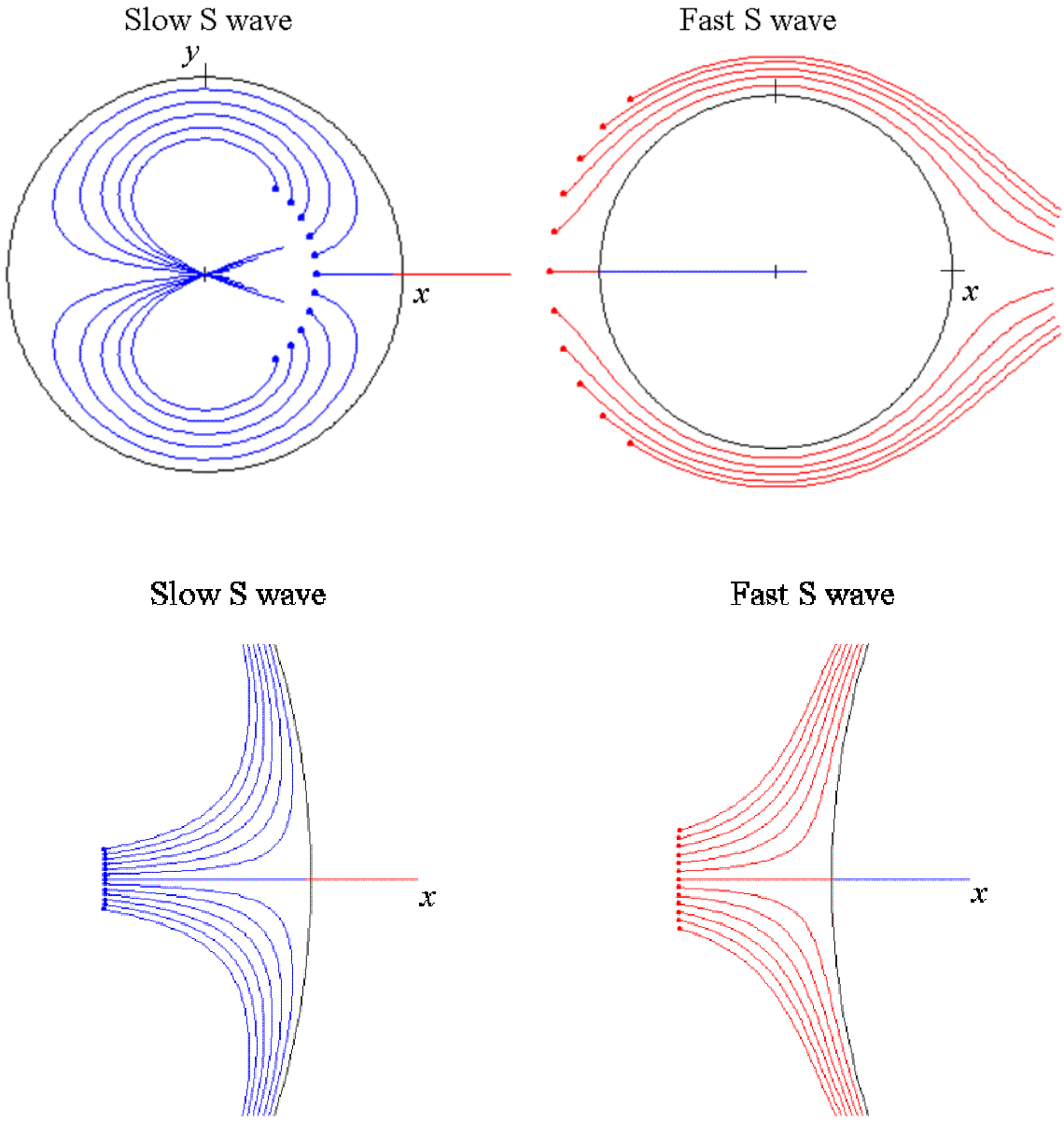

Figure 6. The behaviour of rays of the fast (right) and slow (left) waves near the conical singularity in model (c). The cross marks the vertical axis. The circles mark the anticaustic that corresponds to deviation 26.56° of ray directions from the vertical axis. The full dots mark the initial directions of the rays. The lower plots show a detailed behaviour of rays in a close vicinity of the anticaustic.

The behaviour of rays near the conical singularity is shown in Fig. 6. The form of the ray field is mainly controlled by the anticaustic associated with the conical singularity. The anticaustic distorts rays and causes that the rays cannot touch it. Hence the anticaustic behaves like an obstacle, which must be bypassed. The only rays touching and crossing the anticaustic are rays lying in the *x*-*z* plane. If the ray crosses the anticaustic, the fast wave becomes slow and the slow wave becomes fast. If the ray deviates from the *x*-*z* plane and approaches the anticaustic, it cannot cross the singularity and it is bent (see Fig. 6, lower plots). Hence, the anticaustic separates two domains: the domain of the fast wave that is outside the anticaustic, and the domain of the slow wave that is inside the anticaustic. The rays of the slow wave are captured inside the anticaustic. They are forced not to cross the anticaustic and focused into the point caustic, which is in the centre of the anticaustic. Thus the caustic focuses rays while the anticaustic repels them.

Anisotropy (d) generates eight conical singularities in the following slowness directions

$$\mathbf{n} = \frac{1}{\sqrt{3}}\left(\pm 1, \pm 1, \pm 1\right)^T . \tag{5}$$

The topological charge of polarization vectors in the singularities is 0.5 (see Shuvalov 1998). Anisotropy (d) is rotated so that some of the singularities lie in the *x*-*z* plane (see Fig. 5, lower plots) deviating from the vertical axis by angle $\vartheta = 54.74°$. Anisotropy also forms kiss singularities, two of them are along the vertical axis. The conical singularities generate circular anticaustics. The ray directions at the anticaustic deviate from its centre by angle $\vartheta = 18.41°$. Anisotropy also forms caustics for both *S* waves (see Fig. 7). The pattern of the caustics is more complicated for the slow *S* wave than for the fast *S* wave. The caustics touch the kiss singularities but not the conical singularities. The rays were shot from the source in the following angular interval: $\vartheta = 58°$, $\varphi \in \langle -5°, 5° \rangle$ in steps of 0.5°, where ϑ is the deviation of the slowness vector from the vertical axis, and φ is the polar angle of the slowness vector.

Figure 8 shows equal-area plots of the ray field for both *S* waves. The geometry of rays is affected by caustics crossing the kiss singularity along the vertical axis and by two anticaustics. Likewise in model (c) (Fig. 6), anticaustics represent a barrier for rays. The rays of the fast *S* wave flow around the anticaustic, while the rays of the slow *S* wave are captured inside the anticaustic. The captured rays pass the caustic, which is generated by the conical singularity. Passing the caustic the rays leave the anticaustic domain and the influence of the anticaustic on the rays is lost.

3.3. Wedge singularity

The wedge singularity is defined as the direction in which two slowness sheets touch through the vertices of wedge-shaped surfaces (Shuvalov 1998). The wedge singularity arises from the conical singularity, if one of the semi-axes of the elliptical base of the cone goes to infinity. If

both semi-axes of the cone go to infinity, the conical singularity transforms into the kiss singularity. Hence, the wedge singularity combines properties of the kiss and conical singularities. The wedge singularity generates a linear anticaustic on the wave surface. The linear anticaustic associated with the wedge singularity is, in fact, a degenerated elliptical anticaustic associated with the conical singularity. Since the wedge singularity is always touched by parabolic lines on the slowness sheet of the slow wave, the anticaustic is touched by the caustic at two points on the wave surface.

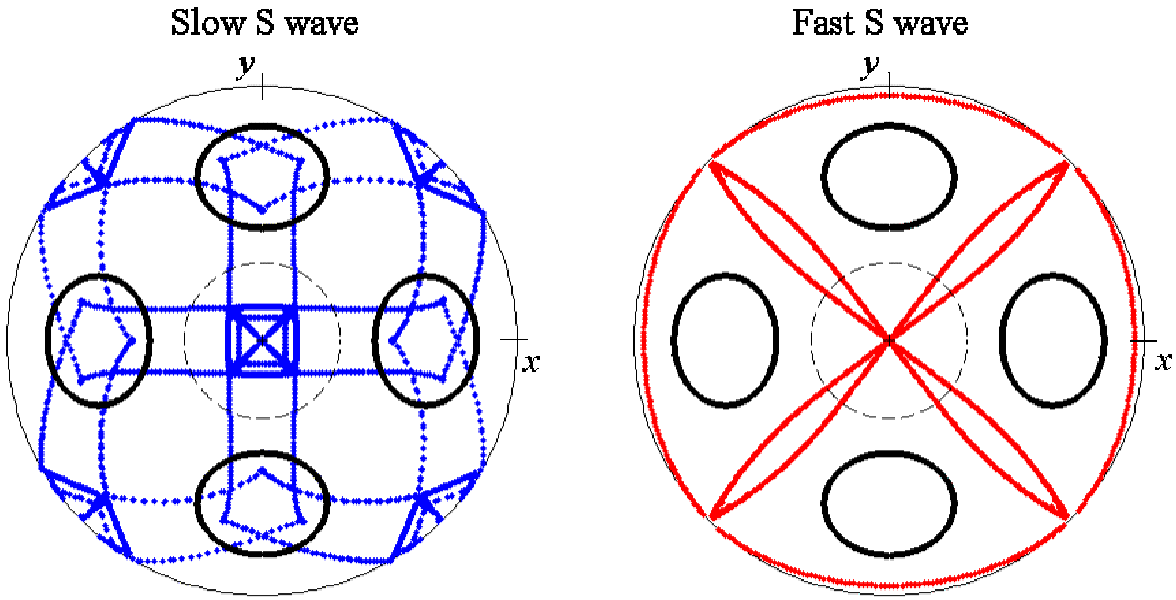

Figure 7. Caustics on the wave sheets for the *S*1 (right) and *S*2 (left) wave in anisotropic model (d) displaying cubic symmetry. The ellipses mark anticaustics. The inner/outer circles correspond to deviation 25°/90° of ray directions from the vertical axis. The kiss singularity coincides with the vertical axis.

The behaviour of rays near the wedge singularity is studied in a model displaying a triclinic anisotropy (see Fig. 9). The triclinic anisotropy arose by a perturbation of the cubic anisotropy by adding a non-zero parameter a_{25}. The anisotropy model is inhomogeneous with constant velocity gradient $\varepsilon = 0.01$ along the *x*-axis. The source of wave is situated at the origin of coordinates. The elastic parameters are at the source: $a_{11} = a_{22} = a_{33} = 6.25$, $a_{44} = a_{55} = a_{66} = 2.08$, $\gamma = a_{12} - a_{11} + 2a_{44} = 2.00$ and $a_{25} = 1.00$. The remaining parameters are zero. The elastic parameters at other points of the medium were calculated using Eq. (5).

The studied anisotropy generates the wedge singularity along the vertical axis. The topological charge of polarization vectors in the singularity is 0. The shapes of the slowness and wave sheets illustrate very exceptional properties of the wedge singularity (see Fig. 9). While the slowness sheets of *S* waves touch tangentially in the *x*-*z* plane, they touch through the vertices of two wedges in the *y*-*z* plane. The linear anticaustic associated with the singularity is along the *y*-axis. The anticaustic is touched at its edges by caustics. The rays were shot from the source in the following angular interval: $\vartheta = 10°$, $\varphi \in \langle -5°, 5° \rangle$ in steps of 1°, where ϑ is the deviation of the slowness vector from the vertical axis, and φ is the polar angle of the slowness vector.

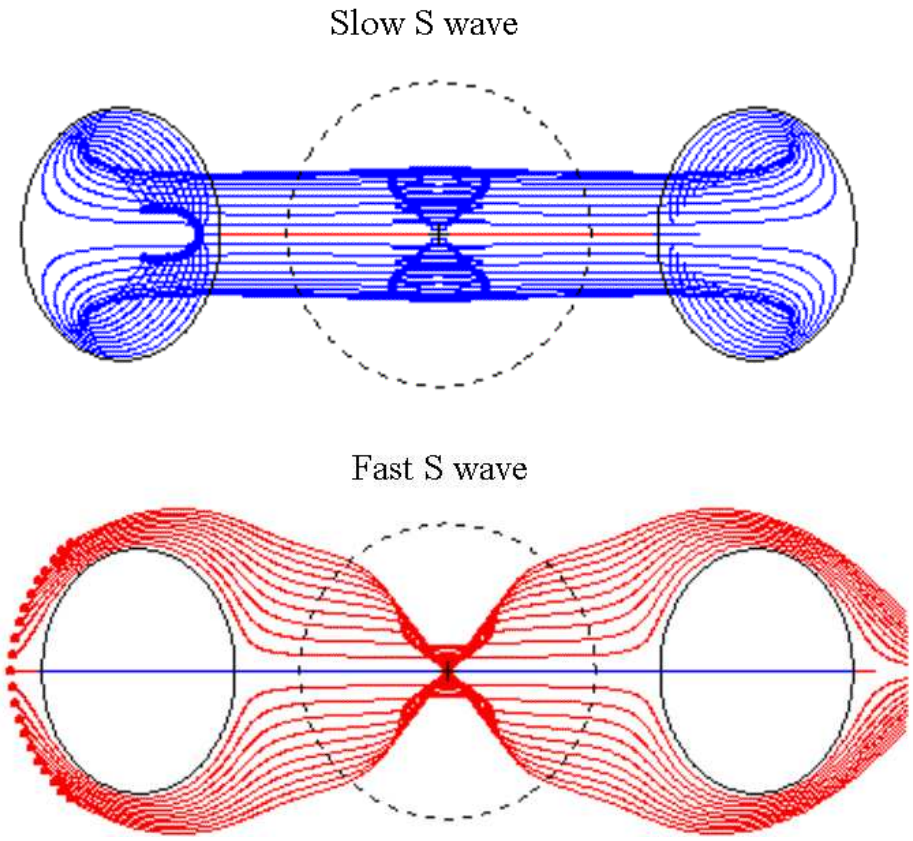

Figure 8. The behaviour of rays of the fast *S* (lower plot) and slow *S* (upper plot) waves in model (d). The cross marks the kiss singularity that coincides with the vertical axis. The ellipses mark anticaustic associated with conical singularities The full dots mark the initial directions of the rays. The inner circle corresponds to deviation 25° of ray directions from the vertical axis.

Figure 10 shows equal-area plots of the ray field for both *S* waves. Likewise for the conical singularity, the geometry of rays is strongly affected by presence of the anticaustic. The anticaustic prevents rays from following simply the gradient direction and deflects them not to cross but move around the anticaustic. The rays are bend and focused at the edges of the anticaustic, where the anticaustic is touched by the caustic. Behind the anticaustic, the rays are forced to pass a cusped edge of the anticaustic, which lies in the *x*-*z* plane. The only rays not affected by the anticaustic are rays in the *x*-*z* plane.

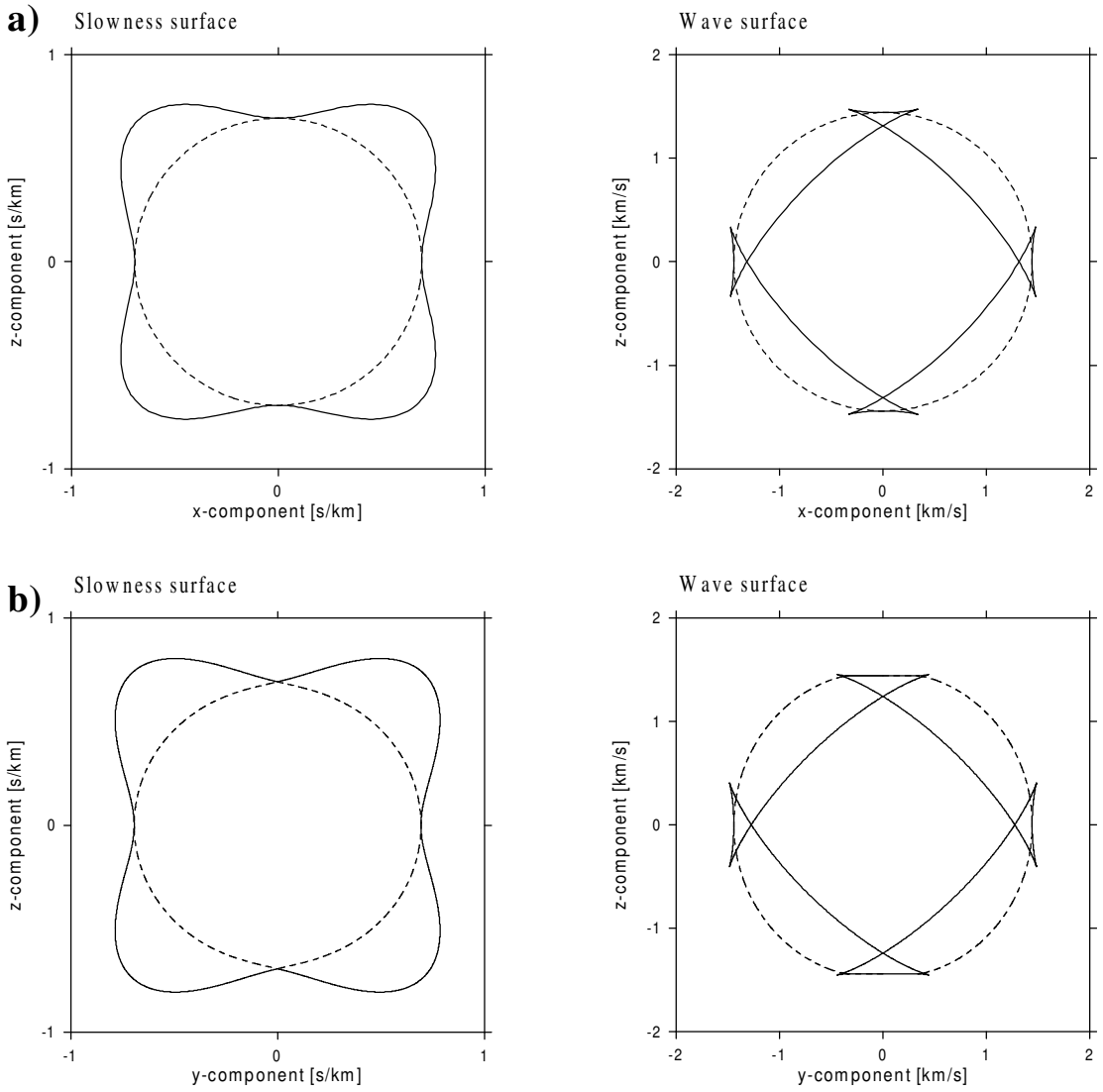

Figure 9. The sections of the slowness and wave surfaces for triclinic anisotropy in the *x*-*z* (a) and *y*-*z* (b) planes. The dashed and full lines denote the slowness and wave sheets of the fast and slow waves, respectively. For parameters of the model, see the text.

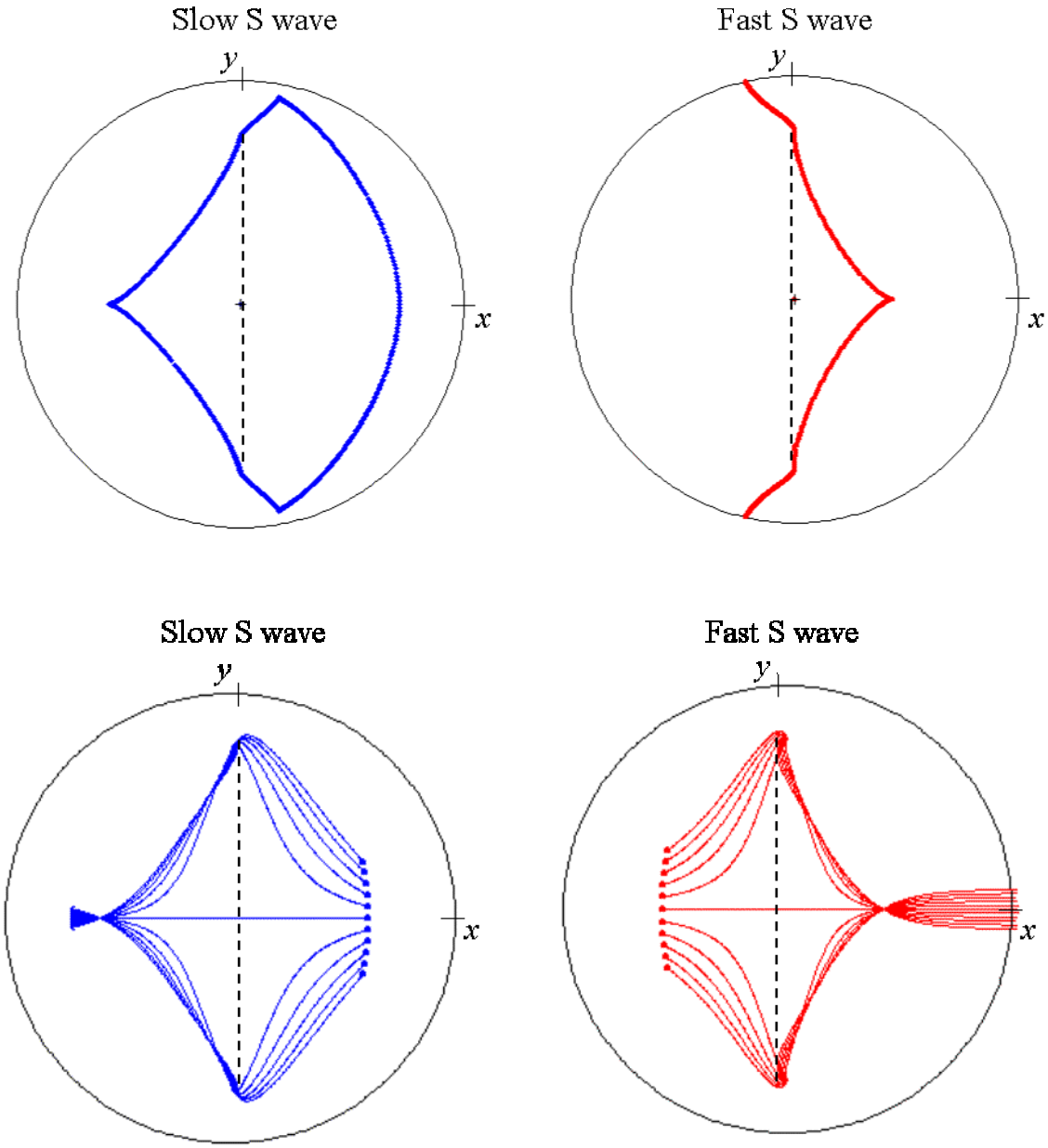

Figure 10. Caustics on the wave sheets (upper plots) and the behaviour of rays (lower plots) of the fast *S* (right) and slow *S* (left) waves near the wedge singularity in triclinic anisotropy. The cross denotes the vertical axis. The dashed line marks the anticaustic associated with the wedge singularity. The full dots mark the initial directions of the rays. The circles correspond to deviation 18° of ray directions from the vertical axis.

4. DISCUSSION

The behaviour of rays can display a complicated pattern in inhomogeneous anisotropic media. The ray field is not affected only by the velocity gradient as in isotropic media but also by the symmetry and strength of anisotropy. The anisotropy can strongly affect the ray fields and introduce effects, which cannot be observed under isotropy. For example, while the rays are 2-D (planar) curves in 1-D inhomogeneous isotropic media, the rays can form complicated 3-D curves in 1-D inhomogeneous anisotropic media. While the bending of rays follows the direction of the velocity gradient in isotropic media, the bending of rays may significantly deviate from the direction of the velocity gradient in anisotropic media. For concave areas on the slowness surface, one can even observe the bending of rays, which is quite opposite to the direction of the velocity gradient.

Peculiarities in the behaviour of rays can also be induced by singularities in anisotropy. It concerns namely the conical and wedge singularities. These singularities generate caustics and anticaustics in their vicinity that play an essential role in forming the ray field. The role of the anticaustic in forming the ray field is particularly interesting. The anticaustic prevents rays from following simply the gradient direction in the medium and deflects them not to cross it. Hence the anticaustic behaves like a barrier for a ray. The anticaustic of the wedge singularity is linear and the rays move around it. The anticaustic of the conical singularity is elliptical or circular and separates two domains: the domain of the fast wave that is outside the anticaustic, and the domain of the slow wave that is inside the anticaustic. The rays outside the anticaustic move around it, while the rays inside the anticaustic are captured. The captured rays are forced to pass the caustic generated by the conical singularity. Passing the caustic the influence of the anticaustic on the rays is lost. One can observe that the anticaustic is also crossed by a ray, but only in very exceptional cases. If the ray passes the anticaustic, the slow wave becomes fast and the fast wave becomes slow. The anomalies in the ray behaviour due to singularities are more pronounced under strong anisotropy, if anisotropy decreases the ray field becomes more regular.

Acknowledgements

I thank V. Červený for stimulating discussions on the subject. The work was supported by the Consortium Project “Seismic waves in complex 3-D structures”, and by the Grant Agency of the Czech Republic, grant No. 205/00/1350.

References

Aki, K. & Richards, P.G., 1980. *Quantitative Seismology. Theory and Methods*, W.H. Freeman, San Francisco.

Alshits,V.I., Sarychev, A.V. & Shuvalov, A.L., 1985. Classification of the degenerations and analysis of their stability in elastic wave theory in crystals, *J. Exper. Theor. Phys.*, **89**, 922-938 (in Russian).

Červený, V., 1972. Seismic rays and ray intensities in inhomogeneous anisotropic media, *Geophys. J. R. astr. Soc.*, **29**, 1-13.

Červený, 2001. *Seismic Ray Theory*, Cambridge University Press, Cambridge.

Červený, V., Molotkov, I.A. & Pšenčík, I., 1977. *Ray Method in Seismology*, Charles University Press, Praha.

Grechka, V.Yu. & Obolentseva, I.R., 1993. Geometrical structure of shear wave surfaces near singularity directions in anisotropic media, *Geophys. J. Int.*, **115**, 609-616.

Payton, R.G., 1992. Wave propagation in a restricted transversely isotropic elastic solid whose slowness surface contains conical points, *Q. J. Mech. Appl. Math.*, **45**, 183-197.

Pšenčík, I. & Dellinger, J., 2001. Quasi-shear waves in inhomogeneous weakly anisotropic media by the quasi-isotropic approach: a model study, *Geophysics*, **66**, 308-319.

Rümpker, G. & Thomson, C. J., 1994. Seismic-waveform effects of conical points in gradually varying anisotropic media, *Geophys. J. Int.*, **118**, 759-780.

Shuvalov, A.L., 1998. Topological features of the polarization fields of plane acoustic waves in anisotropic media, *Proc. R. Soc. Lond.*, **A 454**, 29112947.

Shuvalov, A.L. & Every, A.G., 1996. Curvature of acoustic slowness surface of anisotropic solids near symmetry axes, *Phys. Rev.*, **B 53**, No. 22, 14.906-14.916.

Shuvalov, A.L. & Every, A.G., 1997. Shape of the acoustic slowness surface of anisotropic solids near points of conical degeneracy, *J. Acoust. Soc. Am.*, **101**, 2381-2382.

Vavryčuk, V., 1999. Properties of *S* waves near a kiss singularity: a comparison of exact and ray solutions, *Geophys. J. Int.*, **138**, 581-589.

Vavryčuk, V., 2001. Ray tracing in anisotropic media with singularities, *Geophys. J. Int.*, **145**, 265-276.

Vavryčuk, V., 2002. Asymptotic elastodynamic Green function in the kiss singularity in homogeneous anisotropic solids, *Stud. Geophys. Geod.*, **46**, 249-266.